ELSEVIER

Journal of Alloys and Compounds 323–324 (2001) 4–7

Journal of ALLOYS AND COMPOUNDS

www.elsevier.com/locate/jallcom

Formation and structure of highly over-stoichiometric $LaNi_{5+x}$ (x~1) alloys obtained by manifold non-equilibrium methods

F. Cuevas[a,*], M. Latroche[a], M. Hirscher[b], A. Percheron-Guégan[a]

[a]*Laboratoire de Chimie Métallurgique des Terres Rares, ISCSA-CNRS, 2–8 rue Henri Dunant, 94320 Cedex, France*
[b]*Max-Planck-Institut für Metallforschung, Heisenbergstrasse 1, D-79569 Stuttgart, Germany*

Abstract

Highly over-stoichiometric $LaNi_{5+x}$ (x~1) alloys have been obtained by distinct non-equilibrium preparation routes: ageing of amorphous La–Ni films, melt spinning and mechanical alloying. These alloys are metastable and exhibit a $TbCu_7$-type structure. Refinement of X-ray diffraction data show that overstoichiometry is achieved by a random substitution of some La atoms by c-axis oriented Ni dumbbells followed by a relaxation of basal Ni atoms towards the dumbbell position. Annealing of $LaNi_{5+x}$ (x~1) alloys at moderated temperatures (~800 K) produces precipitation of the secondary Ni phase as dictated by the La–Ni equilibrium phase diagram. We propose that metastable La–Ni alloys with $TbCu_7$-type structure are formed when the atomic mobility in the system is low enough to prevent the diffusion of Ni atoms towards Ni-precipitation centers. The possibility of preparing these compounds by mechanical alloying enables their production on a large scale for possible industrial applications.

Keywords: Intermetallics; Hydrogen storage materials; Mechanical alloying; X-ray diffraction

1. Introduction

The $LaNi_5$ alloy is known to be an outstanding material for hydrogen storage, since it absorbs reversibly about one hydrogen per metal atom. Unfortunately, stoichiometric $LaNi_5$ has a poor cycling stability for battery applications, which is currently solved by partial replacement of nickel by Mn, Al and costly Co. Recent investigations show that a high electrochemical cycling stability can also be attained in Co-free over-stoichiometric compounds. $La(Ni_{1-z}M_z)_{5+x}$ alloys with M=Cu (x=1) [1] and Mn (x~0.6) [2] present very good cycle-lifes due to their reduced discrete lattice expansion accompanying hydride formation.

The Ni-rich portion of the binary La–Ni phase diagram [3] presents an homogeneous region with composition $LaNi_{5+x}$ in the range of $-0.15<x<0.4$ at 1543 K. Overstoichiometry occurs by the formation of a $TbCu_7$-type structure but seems to be limited to x=0.4 in the equilibrium state. Nevertheless, the preparation of highly over-stoichiometric $LaNi_{5+x}$ ($1<x<4$) metastable alloys by ion beam sputtering (IBS) [4] has been recently published. Unfortunately, sputtering methods do not allow production of sufficient amounts of material for industrial applications. In this work, we report on the feasibility of preparing $LaNi_{5+x}$ (x~1) alloys by other non-equilibrium methods such as ageing of amorphous films, melt-spinning and mechanical alloying (MA).

2. Experimental

La–Ni amorphous films were deposited by IBS onto Al_2O_3-sapphire substrates using a mosaic target of La (99.9% purity) and Ni (99.99% purity) with a Ni surface area of 76%. Film deposition was accomplished using an argon ion beam in a vacuum chamber with a base pressure of 10^{-8} Torr. The substrate temperature and argon pressure in the chamber were kept at 325 K and $5\cdot10^{-5}$ Torr, respectively. Films were deposited at a growth rate of 1.7 Å/s to reach a final thickness of 1.3 μm. Electron probe microanalyses give a film composition of $LaNi_{6.1}$. The amorphous state of these films was proved by the absence of well-defined reflections in electron diffraction patterns obtained by transmission electron microscopy (Phillips CM-20, 200 kV). Films were then annealed in a radiation oven for 30 min at distinct temperatures within the range 625–925 K. The crystal structure of the annealed films was

*Corresponding author.
E-mail address: fermin.cuevas@glvt-cnrs.fr (F. Cuevas).

0925-8388/01/$ – see front matter
PII: S0925-8388(01)01004-0

studied by X-ray diffraction (XRD) using a CuKα Bragg–Brentano diffractometer equipped with a secondary monochromator.

Melt-spun samples were prepared by quenching 10 g of a molten ingot alloy with $LaNi_7$ composition over a Cu-wheel having a surface velocity of 25 m/s. The initial ingot was produced by arc-melting of the constituting elements. Melt-spinning was conducted under a 100 mbar He (99.996% purity) atmosphere. The temperature of the alloy for injection was about 1700 K. The obtained samples were mostly in the form of ribbons, 35 μm in thickness and 2 mm in width. However, a small amount of material was also obtained in the form of wires, 0.3 mm in diameter, resulting from the end of the injection process. The crystal structure of the initial ingot and melt-spun ribbons and wires were analysed using the XRD equipment described above.

In order to get powder La–Ni samples by MA, an 8-g ingot with $LaNi_7$ composition was initially prepared by induction melting starting from the pure elements. The ingot was mechanically crushed down to 1-mm particle size and then introduced into a stainless steel ball-milling bowl. MA was carried out in a Fritsch P7 planetary ball mill for 65 h at a milling speed of 500 rpm. The La–Ni alloy mass to ball ratio was 1:10, and the balls were 14 mm in diameter. Some of the mechanically alloyed powder was then cold pressed at 10 ton cm^{-2} and then annealed for 1 h at 775 K in secondary vacuum to improve its crystallinity. XRD measurements were performed for these samples in a Bruker AXS D8 Advance θ–θ diffractometer equipped with a secondary monochromator using CuKα radiation. The resulting XRD patterns have been analysed by the Rietveld method using the FULLPROF program [5].

3. Results and discussion

XRD patterns within the representative 2θ range of 30–50° from as-deposited and 625-, 875- and 925-K-annealed La–Ni films are displayed in Fig. 1. The as-deposited film shows no reflections due to its amorphous structure. The crystallisation onset of amorphous La–Ni occurs in the temperature range between 325 and 625 K in agreement with Knoll [6], who established a crystallisation temperature at about 500 K for amorphous La–Ni films of similar composition. Peak reflections from the 925-K-annealed film have been indexed to two phases: an hexagonal $P6/mmm$ structure and fcc-Ni. On increasing the annealing temperature, ($hk0$) reflections shift to lower angles, whereas ($00l$) reflections undergo the opposite behaviour, i.e. the a axis of the hexagonal structure expands and the c axis contracts. This variation of lattice parameters is typical of common over-stoichiometric $LaNi_{5+x}$ alloys when x decreases [3,4,7]. Over-stoichiometry occurs by the formation of the so-called $TbCu_7$ structure, which consists on the partial and random substitution of La atoms by Ni dumbbells, as displayed in Fig. 2, in the $CaCu_5$-type structure. Besides, the intensity of the Ni peak ($2\theta \sim 44.5°$), which is practically negligible at 625 K, gradually increases with the annealing temperature. Hence, it can be inferred that a single $LaNi_{5+x}$-phase occurs at the crystallisation onset of amorphous films. Afterwards, on increasing the annealing temperature, Ni progressively segregates out of the $LaNi_{5+x}$-phase. Regarding the initial composition of the amorphous film, it is concluded that a highly over-stoichiometric $LaNi_{5+x}$ alloy with $x \sim 1$ is formed by annealing amorphous La–Ni films at 625 K. This conclusion concurs with that of Ref. [6].

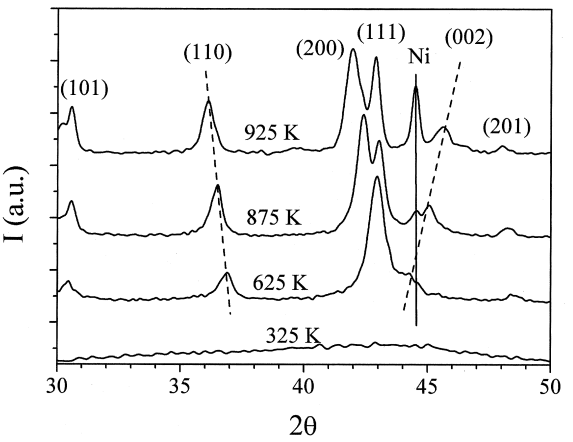

Fig. 1. XRD diffraction patterns of as-deposited (325 K) and annealed La–Ni films obtained by IBS. The shifts of (110) and (002) reflections, related to the $LaNi_{5+x}$-phase, are indicated by dashed lines. The position of the (111)-Ni reflection is indicated by a continuous line.

XRD patterns of melt-spun ribbons present a two-phase $LaNi_{5+x}$ + Ni behaviour consistent with the La–Ni phase equilibrium diagram. However, some additional reflections are observed at the same positions as those registered for the previous $LaNi_{5+x}$ ($x \sim 1$) film. These reflections are

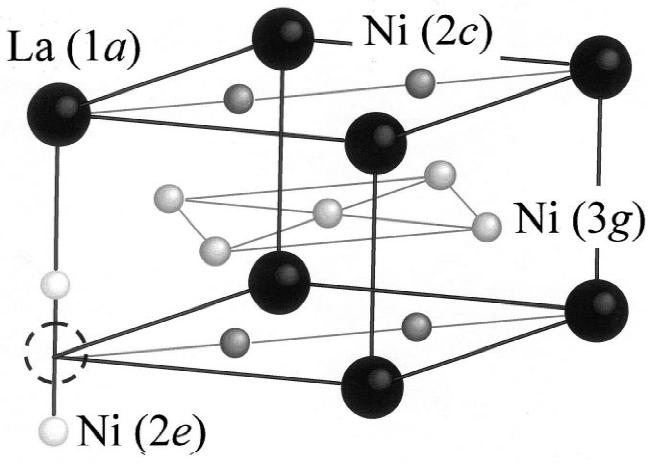

Fig. 2. Substitution of a La atom by a Ni dumbbell in the unit $CaCu_5$-type cell. This random substitution, without long range order, leads to the $TbCu_7$ structure. Sites for Ni and La atoms are given according to the Wickoff description.

predominant for wires and maybe ascribed to the partial formation of highly over-stoichiometric $LaNi_{5+x}$ phase. High overstoichiometry only occurs at the material regions where fast enough cooling rates are achieved, i.e. presumably at the ribbon surface facing the Cu-wheel and in residual wires. Thus, although we got evidence that high overstoichiometry in $LaNi_{5+x}$ alloys can be achieved by melt spinning, the preparation conditions employed failed to produce homogeneous materials.

Fig. 3 displays the XRD patterns of La–Ni alloys before and after MA within the representative 2θ range of 25–55°. The non-annealed MA powder exhibits a nanocrystalline diffraction pattern related to the $LaNi_{5+x}$ phase without any clear presence of Ni reflections. Once again ($hk0$) reflections are shifted to higher angles, whereas ($00l$) reflections move to lower angles in comparison with the conventionally prepared ingot alloy. A similar pattern is observed for the annealed MA powder but the diffraction peaks are slightly sharper and the Ni reflections start to appear. Using the Scherrer approximation, an enlargement from 10 to 40 nm in the crystalline grain size of the $LaNi_{5+x}$ phase is calculated to be produced by the annealing treatment.

The crystallinity of the annealed sample was good enough to perform Rietveld analysis of the whole diffraction pattern ($20° < 2\theta < 100°$, Fig. 4). $LaNi_{5+x}$ and Ni phases have been considered for the refinement. The assumed structural model for the $LaNi_{5+x}$ phase is based on the $CaCu_5$-type structure (space group $P6/mmm$, La in 1*a* (0,0,0); Ni in 2*c* (1/3, 2/3, 0) and 3*g* (1/2, 0, 1/2)) with part of the La atoms replaced by Ni dumbbells occupying the site 2*e* and oriented along the *c* axis. The basal Ni atoms shrink towards the Ni dumbbell to occupy a new 6*l* position. With this configuration, all the crystallographic sites are partially occupied with an occupation factor τ_i, except the 3*g* site, which is considered to be

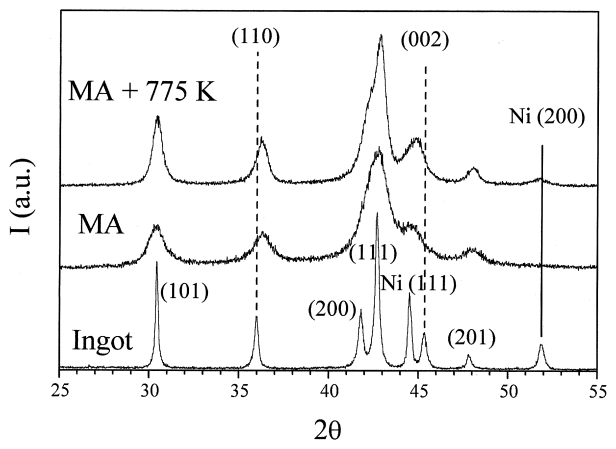

Fig. 3. XRD diffraction patterns of the induction-melted $LaNi_7$ ingot, MA powder and 775-K-annealed MA powder. (110)- and (002)- reflections of the $LaNi_{5+x}$ phase and (200) reflection of the Ni phase are expressly indicated for the ingot pattern by dashed and continuous lines, respectively.

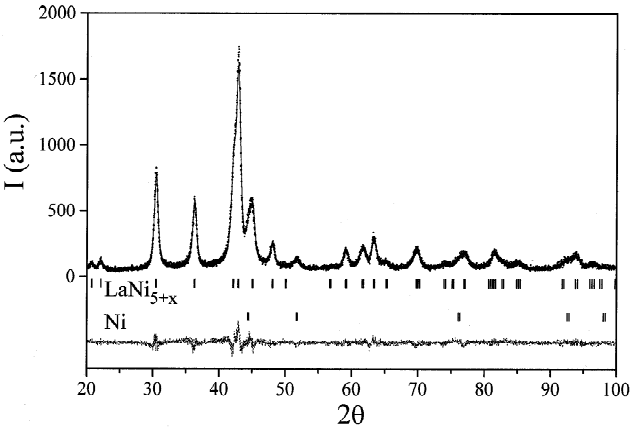

Fig. 4. Refined XRD diffraction pattern of 775-K-annealed MA powder. The observed (dots), calculated (solid line) and difference curves (below) are shown. Vertical bars correspond to peak positions of $LaNi_{5+x}$ and Ni phases. The composition of the $LaNi_{5+x}$ phase, as results from the refined occupancy factors in the Rietveld analysis, is $LaNi_{6.08}$.

unaffected and fully occupied ($\tau_3 = 3$). The values of the site occupancies with $\tau_i \neq 3$ are interrelated and constrained by the fact that La atoms are always replaced by Ni dumbbells to provide over-stoichiometry. Hence, site occupancies can be refined with only one parameter. Such stoichiometric model was first proposed for $YbCu_{6.5}$ by Hornstra and Buschow [8] and corroborated by joint neutron and synchrotron measurements for $LaNi_{5.4}$ by Latroche et al. [9].

The results of the Rietveld refinement are given in Table 1. The low values obtained for χ^2 (1.44) and for the R_{F1} factor (2.28%) indicate the good quality of the refinement and the right assignation of the structural model for the $LaNi_{5+x}$ phase. Moreover, from the obtained *z* coordinate for the 2*e*-Ni (0.312(5)) site, a distance of 2.51(4) Å can be calculated for the two Ni atoms forming the dumbbells, in agreement with the sum of two atomic radii of nickel ($r_{Ni} = 1.246$ Å). The refined occupancy factors of the La and Ni positions in the $LaNi_{5+x}$ phase give a composition of $LaNi_{6.08(5)}$. This value is in agreement with the segregated amount of secondary Ni phase (8.9(2) wt.%), which implies a composition of $LaNi_{6.16(3)}$ for the major phase, as can be deduced from the starting composition of the initial ingot ($LaNi_7$) and the mass conservation law. Furthermore, taking into account the reported linear evolution of both *a* and *c* lattice parameters on the Ni overstoichiometry [7], an average composition of $LaNi_{6.18}$ is obtained. Therefore, it can be concluded from the structural refinement, the lattice parameters and the mass conservation law that the composition for the major phase is close to $LaNi_{6.1}$ which cannot be reached by classical metallurgical elaboration.

To summarise, we have shown that highly over-stoichiometric $LaNi_{5+x}$ alloys with $x \sim 1$ can be prepared by manifold non-equilibrium methods. Such methods involve a highly disordered La–Ni precursor, either in the solid

Table 1
Structural data of MA+775 K annealed La–Ni alloy: atomic coordinates (x, y, z), displacement factors (B) and refined occupancy factors (τ_i)

Site	Atom	x	y	z	B (Å^2)	τ_i
1*a*	La	0	0	0	1.52(8)	$\tau_1=0.866(6)$
2*c*	Ni	1/3	2/3	0	1.02(6)	$\tau_2=1.198(6)$
3*g*	Ni	1/2	0	1/2	1.02(6)	$\tau_3=3$(fixed)
6*l*	Ni	0.286(2)	2x	0	1.02(6)	$\tau_4=0.802(6)$
2*e*	Ni	0	0	0.312(5)	1.02(6)	$\tau_5=0.267(6)$
	R_{wp}	R_p	R_{F1}	R_{F2}	χ^2	N_{ref}
	15.4%	13.4%	2.28%	3.25%	1.44	61
18 variables	*P*6/*mmm*	Cell parameters	$a=4.958(1)$ Å $c=4.030(1)$ Å			$LaNi_{6.08(5)}$
Secondary phase		$Fm\bar{3}m$	$a=3.537(1)$ Å			Ni (8.9(2) wt.%)

state for MA and amorphous films, in the liquid state for melt-spinning, or in the gaseous state for crystalline IBS films [4]. The formation of a single $LaNi_{5+x}$ phase with $TbCu_7$-type structure at the crystallisation onset of the precursor reveals the existence of a local minimum of the Gibbs free energy for the $LaNi_{5+x}$ configuration. If the kinetic energy in the system is high enough, this configuration evolves towards the two phase equilibrium configuration dictated by the La–Ni phase diagram. Therefore, $LaNi_{5+x}$ alloys with $x\sim1$ are metastable. This behaviour is schematically depicted in Fig. 5. Initially, the formation of the metastable $TbCu_7$ is favoured since this requires only a local rearrangement of the Ni atoms into dumbbells. Later on, annealing to higher temperatures facilitates the long-range diffusion of Ni atoms and nucleation of nickel precipitates occurs.

4. Conclusions

The nickel over-stoichiometry limit in $LaNi_{5+x}$ alloys can be increased from classical values of $x=0.4$ obtained by conventional metallurgy to $x\sim1$ by using non-equilibrium techniques. Such highly overstoichiometric alloys are metastable and adopt the same $TbCu_7$ crystal structure as conventional overstoichiometric alloys. Highly overstoichiometric $LaNi_{5+x}$ alloys can be produced in significant amounts by MA, which enables the production of this material for potential industrial applications.

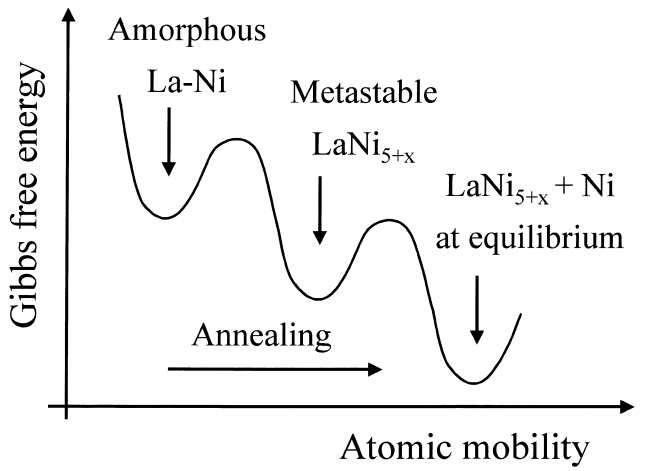

Fig. 5. Schematic representation of the phase configuration evolution in the La–Ni system with global composition $LaNi_6$ as a function of the atomic mobility.

Acknowledgements

The authors wish to thank F. Briaucourt, B. Ludescher and F. Mehner for technical assistance. F. Cuevas is grateful to the Spanish Government and the European Community for financial support.

References

[1] P.H.L. Notten, J.L.C. Daams, R.F.E. Einerhand, J. Alloys Comp. 210 (1994) 233.
[2] P.H.L. Notten, M. Latroche, A. Percheron-Guégan, J. Electrochem. Soc. 146 (1999) 3181.
[3] K.H.J. Buschow, H.H. Van Mal, J. Less-Common Met. 29 (1972) 203.
[4] F. Cuevas, M. Hirscher, B. Ludescher, H. Kronmüller, J. Appl. Phys. 86 (1999) 6690.
[5] J. Rodriguez-Carvajal, Union of Crystallography, in: Abstract of Satellite Meeting on Powder Diffraction, Toulouse, France, 1990, p. 127.
[6] R.W. Knoll, Mater. Lett. 3 (4) (1985) 137.
[7] P.H.L. Notten, J.L.C. Daams, R.E.F. Einerhand, Ber. Bunsenges. Phys. Chem. 96 (1992) 656.
[8] J. Hornstra, K.H.J. Buschow, J. Less-Common Met. 27 (1972) 123.
[9] M. Latroche, J.-M. Joubert, A. Percheron-Guégan, P.H.L. Notten, J. Solid State Chem. 146 (1999) 313.